amcs

COOPERATIVE CONVEX CONTROL OF MULTIAGENT SYSTEMS APPLIED TO DIFFERENTIAL DRIVE ROBOTS

FRANCISCO-RONAY LÓPEZ-ESTRADA [a], HELEN DARIAS [a], VICENÇ PUIG [b],
GUILLERMO VALENCIA-PALOMO [c,*], JOAQUÍN DOMÍNGUEZ-ZENTENO [a],
MARÍA-EUSEBIA GUERRERO-SÁNCHEZ [c]

[a]TURIX-Dynamics—Diagnosis and Control Group
National Technological Institute of Mexico
IT Tuxtla Gutiérrez, Carr. Panamericana Km. 1080, SN, 29050, Tuxtla Gtz, Mexico
e-mail: {frlopez,m20270380,joaquin.dz}@tuxtla.tecnm.mx

[b]Institute of Robotics and Industrial Informatics
Polytechnic University of Catalonia
C/Llorens i Artigas 4-6, 08028, Barcelona, Spain
e-mail: vicenc.puig@upc.edu

[c]IIxM CONAHCYT & TURIX-Dynamics—Diagnosis and Control Group
National Technological Institute of Mexico
IT Hermosillo, Av. Tecnológico 115, 83170, Hermosillo, Mexico
e-mail: {gvalencia,maria.guerreros}@hermosillo.tecnm.mx

This work proposes a convex cooperative control scheme for a multiagent system of differential mobile robots in a leader–follower formation. First, the kinematic model of the differential robots is obtained in a linear parameter varying representation. Next, a reference model approach is considered to track the desired trajectory. The paper's contribution is then to derive conditions to guarantee the convergence of the convex controller, which is achieved using a non-quadratic Lyapunov function. Subsequently, this control law is integrated into the agent that leads a distributed control protocol based on graph theory designed to reach the consensus of the followers. Simulations of five mobile robots are performed to illustrate the effectiveness of the proposed method.

Keywords: convex control, multiagent system, differential robots, tracking control.

1. Introduction

The consensus problem of multiagent systems (MASs) has been a topic of interest in recent decades due to its potential applications in industry, aeronautics, and search and rescue. An example was seen recently during the Tokyo Olympics, where 1800 aerial drones were synchronized to form the earth's surface. Consensus is a distributed protocol that is related to synchronizing each agent of a network topology by converging its states with those of neighboring agents (Lewis *et al.*, 2013). The consensus state can depend on the interest of all agents (leaderless consensus) or be given by one or

multiple agents (leader–follower consensus). Leaderless and leader-following consensus protocols for MASs can be found in the work of Liu *et al.* (2020), Zhang *et al.* (2021), Ai and Wang (2021), Ahmed *et al.* (2023) or Gong *et al.* (2023).

Regarding the leader-following consensus, some works in the field of MASs have recently been reported. For instance, Ollervides-Vazquez *et al.* (2020) propose a formation control for multiple unmanned aerial vehicles using a sectorial fuzzy controller validated with real experiments on a Parrot ARDrone. Yao *et al.* (2022) dedicated their work to solving the three-dimensional formation problem for multiple aerial robots in environments with obstacles. González-Sierra

et al. (2021) focused on developing ground vehicle formations for precise trajectory tracking. Furthermore, Zhang *et al.* (2022) delved into cooperative attitude control within satellite arrays, further enriching the field. Ahsan Razaq *et al.* (2020) advanced the field by presenting a robust H_∞ leader-based consensus framework capable of rejecting external disturbances and adapting to a switching topology. Complementing this, Rehan *et al.* (2019) and Razaq *et al.* (2023) proposed an innovative approach for observer-based leader-following consensus control, addressing challenges related to input saturation. For a more comprehensive and in-depth exploration of these contributions, interested readers may refer to the recent survey by Amirkhani and Barshooi (2022). In the scope of our work, we focus on a group of differential-drive robots in a leader–follower consensus context. These robots exhibit nonholonomic properties and nonlinear kinematics, adding to the complexity of the multi-agent system.

The collaborative control for differential-drive robots has received attention recently since each robot in the system must autonomously control its velocity and orientation to reach a consensus among all the robots. Some methods used in the literature to achieve this are mentioned next. In the work of Abdulwahhab and Abbas (2018), a fractional-order state feedback controller is designed for trajectory tracking. Dian *et al.* (2019) investigated the trajectory tracking problem for nonholonomic systems with uncertainties using fuzzy and sliding mode techniques, obtaining a robust adaptive controller. González-Sierra *et al.* (2021) focused on control strategies for trajectory tracking based on an extended kinematic model and an observer that predicts the attitudes of each robot of the MAS. In the work of Manoharan and Chiu (2019), a consensus-based control tracks dynamic trajectories for differential robots. A distributed control law for a leader–follower formation is used by Miao *et al.* (2018). Moreno-Valenzuela *et al.* (2022) propose a saturated proportional-integral (PI) controller that provides robustness against disturbances with bounded control signals for a differential robot system to follow a defined trajectory. In the work of Nuno *et al.* (2020), a proportional controller affected by communication delays while each robot seeks to reach a desired position and orientation is presented. Wu *et al.* (2018) design an observer-based controller for a leader–follower formation of two-wheeled robots to avoid obstacles. It is important to note that a critical part of the consensus is controlling the leader robot, as the leader error is transferred to the followers, and most approaches consider linear controllers for this task. However, a more precise leader controller would improve the overall performance.

Controllers based on convex linear parameter varying (LPV) models can improve the leader's performance.

These models comprise a set of local linear models interpolated by scheduling functions. The main advantage of LPV system representations is that powerful linear tools, such as linear matrix inequalities (LMIs), can be used to design controllers for nonlinear systems without the need to handle pure nonlinear models (with their associated complexity) in the design stage. Few works in the literature consider an LPV-based controller approach applied to MASs. For example, Attallah and Werner (2020) proposed an event-triggered formation control for nonholonomic MAS by modeling the dynamics of unicycle robots with an LPV approach. In the work of Saadabadi and Werner (2021), an event-triggered distributed control strategy for a homogeneous nonholonomic MAS is proposed, leading to a set of LMIs that guarantee the controller performance. Subiantoro *et al.* (2020) proposed a distributed LPV model predictive controller for the consensus of a group of mobile robots. In the work of Zakwan and Ahmed (2019), a distributed output feedback control of four differential mobile robots is presented where Lyapunov–Krasovskii functionals were considered to formulate the controller solution regarding LMIs. Recently, Moradi *et al.* (2022) proposed a switching distributed LPV controller for the consensus of LPV multiagent systems applied to a vertical take-off and landing helicopter. Zhu and Tan (2023) introduced an unknown input LPV observer to realize the MAS consensus; however, only a numerical example was considered to validate the method. Although there have been some contributions, the issue remains unresolved, especially for nonholonomic systems, where challenges of uncontrollability persist due to their nonlinear nature.

This work proposes a control strategy that comprises a convex quasi-LPV (qLPV) controller for the leading robot and a MAS distributed control strategy to achieve a consensus among the following robots using graph theory. The first contribution is related to the design of the leader controller, which is based on a reference model of the path following error that splits the controllable and the uncontrollable part. The former is rewritten by hiding the nonlinear terms on the scheduling functions; as a result, a controllable convex qLPV model is obtained. Then, a non-quadratic Lyapunov function is considered to derive a set of feasible linear matrix inequalities that guarantee the performance and convergence of the controller. Second, this control law is integrated into the agent that leads a distributed control protocol based on graph theory designed to reach the consensus of the followers. The goal is for all followers to reach a consensus considering only the information provided by their neighbors. Finally, simulations are performed in a virtual environment developed in Matlab to illustrate the method's effectiveness.

The rest of the paper is organized as follows: Section 2 provides a summary of graph theory and

convex models; Section 3 presents problem formulation; Section 4 is devoted to the convex model derivation of the differential robot and the convex state feedback control law design for the leader agent; Section 5 develops the distributed control protocol of the follower agents; Section 6 shows the results obtained from a numerical example of both the leader and the followers; finally, Section 7 includes the conclusions and outlines future work.

2. Preliminaries

2.1. Graph theory.
Graph theory is used to illustrate the communication and information among the agents. A graph is defined by the pair $\bar{G} = (\bar{R}, \bar{E})$, where $\bar{R} = \{r_0, r_1, \ldots, r_N\}$ is the group of $N + 1$ nodes and $\bar{E} \subseteq (\bar{R} \times \bar{R})$ is a group of edges. $\bar{E}$ is composed of elements (r_i, r_j) representing the connection between nodes r_i and r_j. $\bar{G}$ can be represented by an associated matrix $W = [a_{ij}]$ with weights $a_{ij} > 0$ if $(r_j, r_i) \in \bar{E}$, $a_{ij} = 0$ otherwise, and $a_{ii} = 0$. The weighted in-degree of node r_i is the sum of the elements of the i-th row of W: $d_i = \sum_{j=1}^{N} a_{ij}$, and the diagonal matrix of the graph is $D = \text{diag}\{d_i\}$. We define the Laplacian matrix $L = D - W$. Furthermore, it is necessary to define a diagonal matrix $M = \text{diag}\{m_1, m_2, \ldots, m_n\}$ called the leading adjacency matrix with $m_i \geq 0$ for any i. If the leader is a neighbor of node r_i, then $m_i > 0$; otherwise, $m_i = 0$.

2.2. Convex representation.
Given a nonlinear system $\dot{x}(t) = f(x(t)) + g(x(t))u(t)$, $y(t) = s(x(t))$, it is possible to represent it as a convex Takagi–Sugeno system as follows (Lendek *et al.*, 2011; Bernal *et al.*, 2019):

$$\dot{x}(t) = \sum_{i=1}^{l} \rho_i(\zeta(t))(A_i x(t) + B_i u(t)),$$
$$y(t) = \sum_{i=1}^{l} \rho_i(\zeta(t))(C_i x(t)),$$
(1)

where $x(t) \in \mathbb{R}^n$ is the state vector, $u(t) \in \mathbb{R}^l$ is the input vector, $y(t) \in \mathbb{R}^q$ is the output vector and $\zeta(t) = \begin{bmatrix} \zeta_1(t) & \zeta_2(t) & \ldots & \zeta_p(t) \end{bmatrix}^T \in \mathbb{R}^p$ is the vector of bounded functions that encompass the nonlinearities of the system. $A_i \in \mathbb{R}^{n \times n}$, $B_i \in \mathbb{R}^{n \times l}$ and $C_i \in \mathbb{R}^{q \times n}$ are constant matrices, $\rho_i(\zeta(t))$ are the membership functions that must comply with the convex sum property $\sum_{i=1}^{l} \rho_i(\zeta(t)) = 1$ and $\rho_i(\zeta(t)) \geq 0, \forall i = 1, \ldots, l$, which are defined as follows:

$$\rho_i(\zeta(t)) = \prod_{j=1}^{p} \delta_{ij}(\zeta_j(t)),$$
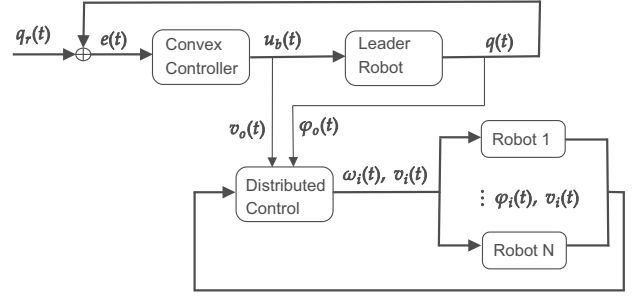(2)

Fig. 1. Collaborative control scheme composed of a convex and a distributed controller.

where $\delta_{ij}(\zeta_j(t))$ is $\eta_0^j(\zeta_j(t))$ or $\eta_1^j(\zeta_j(t))$

$$\eta_0^j((\zeta_j(t)) = \frac{\overline{\zeta_j} - \zeta_j(t)}{\overline{\zeta_j} - \underline{\zeta_j}},$$
$$\eta_1^j((\zeta_j(t)) = 1 - \eta_0^j((\zeta_j(t)),$$
(3)

with $\zeta_j(t) \in [\underline{\zeta_j}, \overline{\zeta_j}]$ being the lower and upper limits of the nonlinearity $\zeta_j(t)$.

3. Problem formulation

The proposed method is illustrated in Fig. 1. It is composed of two controllers. One is a convex qLPV controller for the leader, which considers the trajectory error ($e(t)$) as the controller input. The error is computed from the reference ($q_r(t)$) and the actual ($q(t)$) trajectories of the robot. The controller input ($u_b(t)$) is formed out of the linear ($v(t)$) and angular velocities ($\omega(t)$) such that the leader converges asymptotically to the reference trajectory. The other part is composed of a distributed controller for the follower agents. Graph theory is considered to model communication and interconnection among agents. The next sections elaborate on each of these controllers.

4. Convex controller

4.1. Convex quasi-linear parameter varying (qLPV) model.
Consider a mobile robot as shown in Fig. 2; the kinematic model of the robot is (Blažič and Bernal, 2011)

$$\dot{q}(t) = \begin{bmatrix} \dot{x}(t) \\ \dot{y}(t) \\ \dot{\varphi}(t) \end{bmatrix} = \begin{bmatrix} \cos\varphi(t) & 0 \\ \sin\varphi(t) & 0 \\ 0 & 1 \end{bmatrix} \begin{bmatrix} v(t) \\ \omega(t) \end{bmatrix},$$
(4)

where $(x(t), y(t))$ is the position and $\varphi(t)$ is the orientation of the robot in the plane; $v(t)$ and $\omega(t)$ are the linear and angular velocities, respectively, and $q(t)$ is the vector of generalized coordinates.

The goal is for the robot to follow the desired trajectory, so it is necessary to define the reference

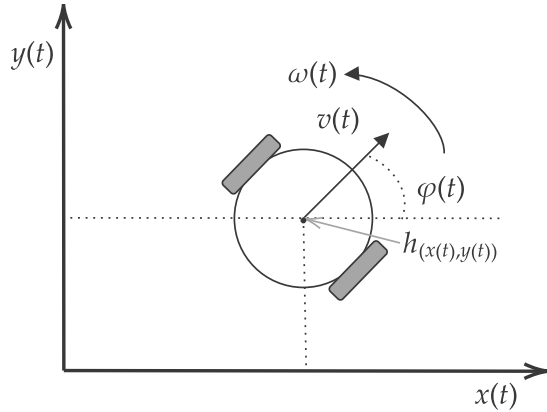$$q_r(t) = [x_r(t) \ y_r(t) \ \varphi_r(t)]^T,$$
(5)

Fig. 2. Diagram of a differential mobile robot.

where $(x_r(t), y_r(t))$ is the desired position and $\varphi_r(t)$ is the desired orientation for the robot, whose dynamic is given by

$$
\begin{aligned}
\dot{x}_r(t) &= v_r(t) \cos \varphi_r(t), \\
\dot{y}_r(t) &= v_r(t) \sin \varphi_r(t), \\
\dot{\varphi}_r(t) &= \omega_r(t),
\end{aligned}
\tag{6}
$$

where $v_r(t), \omega_r(t)$ are the desired linear and angular velocities, respectively, defined by

$$
\begin{aligned}
v_r(t) &= \sqrt{\dot{x}_r^2(t) + \dot{y}_r^2(t)}, \\
\omega_r(t) &= \tan^{-1}\left(\frac{\dot{y}_r^2(t)}{\dot{x}_r^2(t)}\right).
\end{aligned}
\tag{7}
$$

The mathematical model of the tracking error between (5) and $q(t) = [x(t)\ y(t)\ \varphi(t)]^T$ is defined by

$$
\begin{aligned}
e(t) &= R_z(\varphi(t))(q_r(t) - q(t)) \\
&= R_z(\varphi(t)) \begin{bmatrix} x_r(t) - x(t) \\ y_r(t) - y(t) \\ \varphi_r(t) - \varphi(t) \end{bmatrix}.
\end{aligned}
\tag{8}
$$

The rotation matrix about the z-axis is defined as (Corke, 2017)

$$
R_z(\varphi(t)) = \begin{bmatrix} \cos\varphi(t) & \sin\varphi(t) & 0 \\ -\sin\varphi(t) & \cos\varphi(t) & 0 \\ 0 & 0 & 1 \end{bmatrix}.
\tag{9}
$$

Expanding and deriving (8), we have

$$
\begin{aligned}
\dot{e}_x(t) = \omega(t)\big(&-(x_r(t) - x(t))\sin\varphi(t) \\
&+ (y_r(t) - y(t))\cos\varphi(t) \\
&+ (\dot{x}_r(t) - \dot{x}(t))\cos\varphi(t) \\
&+ (\dot{y}_r(t) - \dot{y}(t))\sin\varphi(t),
\end{aligned}
$$

$$
\begin{aligned}
&= \omega(t)e_y(t) + v_r(t)(\cos\varphi_r(t)\cos\varphi(t) \\
&\quad + \sin\varphi_r(t)\sin\varphi(t)) \\
&\quad - v(t)(\cos^2\varphi(t) + \sin^2\varphi(t)), \\
\dot{e}_y(t) &= -\omega(t)((x_r(t) - x(t))\cos\varphi(t) \\
&\quad + (y_r(t) - y(t))\sin\varphi(t)) \\
&\quad - (\dot{x}_r(t) - \dot{x}(t))\sin\varphi(t), \\
&= -\omega(t)e_x(t) + v_r(t)(-\sin\varphi(t)\cos\varphi_r(t) \\
&\quad + \sin\varphi_r(t)\cos\varphi(t)) \\
&\quad - v(t)(\cos\varphi(t)\sin\varphi(t) \\
&\quad - \cos\varphi(t)\sin\varphi(t)), \\
\dot{e}_\varphi(t) &= \omega_r(t) - \omega(t).
\end{aligned}
\tag{10}
$$

The expression (10) can be simplified by using the trigonometric identities

$$
\begin{aligned}
1 &= \cos^2\varphi(t) + \sin^2\varphi(t), \\
\cos(\varphi_r(t) - \varphi(t)) &= \cos\varphi_r(t)\cos\varphi(t) \\
&\quad + \sin\varphi_r(t)\sin\varphi(t), \\
\sin(\varphi_r(t) - \varphi(t)) &= \sin\varphi_r(t)\cos\varphi(t) \\
&\quad - \sin\varphi(t)\cos\varphi_r(t),
\end{aligned}
$$

and $e_\varphi(t) = \varphi_r(t) - \varphi(t)$; then,

$$
\begin{aligned}
\dot{e}_x(t) &= \omega(t)\,e_y(t) + v_r(t)\cos(e_\varphi(t)) - v(t), \\
\dot{e}_y(t) &= -\omega(t)\,e_x(t) + v_r(t)\sin(e_\varphi(t)), \\
\dot{e}_\varphi(t) &= \omega_r(t) - \omega(t).
\end{aligned}
\tag{11}
$$

For convenience, a change of variables is considered to be able to split the non-controllable part of the error model. Then, $\varphi(t)$ is substituted by two new variables:

$$
s(t) = \sin\varphi(t), \quad c(t) = \cos\varphi(t),
$$

whose derivatives are

$$
\begin{aligned}
\dot{s}(t) &= \dot{\varphi}(t)c(t) = c(t)\omega(t), \\
\dot{c}(t) &= -\dot{\varphi}(t)s(t) = -s(t)\omega(t),
\end{aligned}
$$

and the kinematic model (4) becomes

$$
\begin{bmatrix} \dot{x}(t) \\ \dot{y}(t) \\ \dot{s}(t) \\ \dot{c}(t) \end{bmatrix} = \begin{bmatrix} c(t) & 0 \\ s(t) & 0 \\ 0 & c(t) \\ 0 & -s(t) \end{bmatrix} \begin{bmatrix} v(t) \\ \omega(t) \end{bmatrix}.
\tag{12}
$$

The new trajectory errors are

$$
\begin{aligned}
e_x(t) &= c(t)(x_r(t) - x(t)) + s(t)(y_r(t) - y(t)), \\
e_y(t) &= -s(t)(x_r(t) - x(t)) + c(t)(y_r(t) - y(t)), \\
e_s(t) &= s_r(t)c(t) - c_r(t)s(t), \\
e_c(t) &= c_r(t)c(t) + s_r(t)s(t),
\end{aligned}
\tag{13}
$$

and the error dynamics are given by

$$
\begin{aligned}
\dot{e}_x(t) &= \omega\, e_y(t) + v_r(t)e_c(t) - v(t), \\
\dot{e}_y(t) &= -\omega\, e_x(t) + v_r(t)e_s(t), \\
\dot{e}_s(t) &= e_c(t)(\omega_r(t) - \omega(t)), \\
\dot{e}_c(t) &= -e_s(t)(\omega_r(t) - \omega(t)).
\end{aligned}
\tag{14}
$$

The control law is defined as $v(t) = v_r(t)e_c(t) + v_b(t)$, and $\omega(t) = \omega_r(t) + \omega_b(t)$, such that (14) becomes

$$
\begin{aligned}
\dot{e}_x(t) &= e_y(t)\omega_r(t) + e_y(t)\omega_b(t) - v_b(t), \\
\dot{e}_y(t) &= -e_x(t)\omega_r(t) - e_x(t)\omega_b(t) + v_r(t)e_s(t), \\
\dot{e}_s(t) &= -e_c(t)\omega_b(t), \\
\dot{e}_c(t) &= e_s(t)\omega_b(t),
\end{aligned}
\tag{15}
$$

where $u_b(t) = \begin{bmatrix} v_b(t) & \omega_b(t) \end{bmatrix}^T$ is the feedback signal. Note that (15) can be expressed in state-space form as

$$
\begin{bmatrix} \dot{e}_x(t) \\ \dot{e}_y(t) \\ \dot{e}_s(t) \\ \dot{e}_c(t) \end{bmatrix} =
\begin{bmatrix}
0 & \omega_r(t) & 0 & 0 \\
-\omega_r(t) & 0 & v_r(t) & 0 \\
0 & 0 & 0 & 0 \\
0 & 0 & 0 & 0
\end{bmatrix}
\begin{bmatrix} e_x(t) \\ e_y(t) \\ e_s(t) \\ e_c(t) \end{bmatrix}
\\
+ \begin{bmatrix}
-1 & e_y(t) \\
0 & -e_x(t) \\
0 & -e_c(t) \\
0 & e_s(t)
\end{bmatrix}
\begin{bmatrix} v_b(t) \\ \omega_b(t) \end{bmatrix}.
\tag{16}
$$

The model (16) is divided into two subsystems to separate the non-controllable part $\dot{e}_c(t) = e_s(t)\omega_b(t)$, such that the controllable part is given by

$$
\begin{bmatrix} \dot{e}_x(t) \\ \dot{e}_y(t) \\ \dot{e}_s(t) \end{bmatrix} =
\begin{bmatrix}
0 & \omega_r(t) & 0 \\
-\omega_r(t) & 0 & v_r(t) \\
0 & 0 & 0
\end{bmatrix}
\begin{bmatrix} e_x(t) \\ e_y(t) \\ e_s(t) \end{bmatrix}
\\
+ \begin{bmatrix}
-1 & e_y(t) \\
0 & -e_x(t) \\
0 & -e_c(t)
\end{bmatrix}
\begin{bmatrix} v_b(t) \\ \omega_b(t) \end{bmatrix}.
\tag{17}
$$

The model (17) can be converted into a convex qLPV model by choosing ω_r, v_r, e_x, e_y, e_c as nonlinear terms, which are bounded; this is possible because it is assumed that a controller will keep the system close to the desired trajectory. The qLPV is represented through the following form:

$$
\begin{aligned}
\dot{e}(t) &= \sum_{i=1}^{l} \rho_i(\zeta(t))(A_i e(t) + B_i u_b(t)), \\
y(t) &= Ce(t),
\end{aligned}
\tag{18}
$$

where $\zeta(t) = \begin{bmatrix} \omega_r(t) & v_r(t) & e_y(t) & e_x(t) & e_c(t) \end{bmatrix}^T$ contains the nonlinear terms. The intervals of the elements of $\zeta(t)$ are defined according to the physical constraints of the differential mobile robot.

The convex matrices are

$$
A_i = \begin{bmatrix}
0 & \zeta_1(t) & 0 \\
-\zeta_1(t) & 0 & \zeta_2(t) \\
0 & 0 & 0
\end{bmatrix},
\\
B_i = \begin{bmatrix}
-1 & \zeta_3(t) \\
0 & -\zeta_4(t) \\
0 & -\zeta_5(t)
\end{bmatrix}.
$$

Then, by evaluating the state matrices on the bound of the nonlinear term, 32 local models are obtained, which are blended by scheduling functions $\rho_i(\zeta(t))$ defined as

$$
\rho_i(\zeta(t)) = \prod_{j=1}^{5} \delta_j^i(\zeta_j(t)), \quad i = 1, \dots, 32,
$$

$$
\delta_{j_0}^i(\zeta_j(t)) = \frac{\overline{\zeta_j} - \zeta_j(t)}{\overline{\zeta_j} - \underline{\zeta_j}},
$$

$$
\delta_{j_1}^i(\zeta_j(t)) = 1 - \delta_{j_0}^i(\zeta_j(t)), \quad j = 1, \dots, 5.
$$

The scheduling function satisfies the convex property:

$$
\sum_{i=1}^{l} \rho_i(\zeta(t)) = 1, \quad \rho_i(\zeta(t)) \geq 0, \ \ i = 1, \dots, l, \ \ \forall t.
\tag{19}
$$

4.2. Control law. To guarantee the asymptotic convergence of the tracking error, a feedback convex control law is considered for the system (18):

$$
u_b(t) = -\sum_{i=1}^{l} \rho_i(\zeta(t)) F_i e(t),
\tag{20}
$$

such that the closed-loop system is obtained as follows:

$$
\dot{e}(t) = \sum_{i=1}^{l} \sum_{j=1}^{l} \rho_i(\zeta(t))\rho_j(\zeta(t))(A_i - B_i F_j)e(t).
\tag{21}
$$

Typically, quadratic Lyapunov functions are considered to find matrices F_i, but as the number of local models increases, so does conservatism due to a large number of the resulting LMIs. Non-quadratic Lyapunov functions can be considered to address this issue. A non-quadratic Lyapunov function is defined as

$$
V(e(t)) = \sum_{i=1}^{l} \rho_i(\zeta(t))e(t)^T P_i e(t),
\tag{22}
$$

where $P_i = P_i^T > 0$ are unknown constant matrices of suitable dimensions. These functions are a fuzzy combination of multiple quadratic Lyapunov functions. As a result of the non-quadratic Lyapunov function (22), sufficient conditions can be obtained for the asymptotic convergence of the states in the form of LMIs, as described by the following result:

Theorem 1. *If $|\dot{\rho}_\delta| \leq \phi$ holds with $\delta = 1, \ldots, l$, where $|\dot{\rho}_\delta|$ is the modulus of the derivatives of the membership functions, and given the values σ and μ and the matrix G, the closed-loop LPV system (21) with the controller (20) is asymptotically stable if it is possible to obtain the matrices $N, O, K, I, X, S_i = IF_i$ and $P_i = P_i^T > 0$ such that the following is satisfied:*

$$P_\delta - \sum_{i=1}^{l} \frac{P_i}{l} + \frac{X}{l} > 0, \quad \delta = 1, \ldots, l, \quad (23)$$

$$\Psi_i < 0, \quad i = 1, \ldots, r, \quad (24)$$

where

$$\Psi_i = \begin{bmatrix} \psi_{11} & * & * \\ \psi_{21} & O + O^T & * \\ \psi_{31} & \sigma I^T G^T + K - B_i^T O^T & \psi_{33} \end{bmatrix}, \quad (25)$$

with

$$\begin{aligned} \psi_{11} &= \phi X + GS_i + S_i^T G^T - (NA_i + A_i^T N^T), \\ \psi_{21} &= N^T + P_i - OA_i + \sigma GS_i, \\ \psi_{31} &= -B_i^T N^T - KA_i + I^T G^T + \mu S_i, \\ \psi_{33} &= \mu(I + I^T) - KB_i - B_i^T K^T. \end{aligned} \quad (26)$$

Proof. The proof is adopted from the work of Vafamand and Shasadeghi (2017). The time derivative of the Lyapunov function candidate (22) is (to simplify the notation, functional dependencies are removed)

$$\begin{aligned} \dot{V} = &2e^T \left(\sum_{i=1}^{l} \rho_i P_i \right) \dot{e} + e^T \sum_{\delta=1}^{l} \dot{\rho}_\delta \left(P_\delta + \frac{X}{l} - \sum_{i=1}^{l} \frac{P_i}{l} \right) \\ &+ 2\{ e^T N + \dot{e}^T O + u^T K \} \left\{ \dot{e} - \sum_{i=1}^{l} \rho_i \{ A_i e + B_i u \} \right\} \\ &+ 2\{ e^T GI + \dot{x}^T \sigma GI + u^T \mu I \} \left\{ u + \sum_{i=1}^{l} \rho_i F_i e \right\} \\ = &e^T \sum_{\delta=1}^{l} \dot{\rho}_\delta \left(P_\delta + \frac{X}{l} - \sum_{i=1}^{l} \frac{P_i}{l} \right) e + \sum_{i=1}^{l} \rho_i \{ e^T P_i \dot{e} \\ &+ \dot{e}^T P_i e + e^T N \dot{e} + \dot{e}^T N^T e - e^T (NA_i + A_i^T N^T) e \\ &- e^T N B_i u - u^T B_i^T N^T e + \dot{e}^T (O + O^T) \dot{e} - \dot{e}^T O A_i e \\ &- e^T A_i^T O^T \dot{e} - \dot{e}^T O B_i u - u^T B_i^T O^T \dot{e} + u^T K \dot{e} \\ &+ \dot{e}^T K^T u - u^T K A_i e - e^T A_i^T K^T u \\ &- u^T (KB_i + B_i^T K^T) u + e^T GI u + u^T I^T G^T e \\ &+ e^T (GIF_i + F_i^T I^T G^T) e + \dot{e}^T \sigma GI u \\ &+ u^T \sigma I^T G^T \dot{e} + \dot{e}^T \sigma GIF_i e + e^T \sigma F_i^T I^T G^T \dot{e} \\ &+ u^T \mu(I + I^T) u + u^T \mu IF_i e + e^T \mu F_i^T I^T u \}. \quad (27) \end{aligned}$$
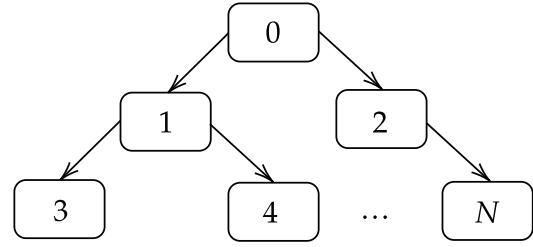

Fig. 3. Graph of the multiagent system.

Assuming that (23) and (24) hold, we get

$$\begin{aligned} \sum_{\delta=1}^{l} \rho_\delta &\left(P_\delta + \frac{X}{l} - \sum_{i=1}^{l} \frac{P_i}{l} \right) \\ &\leq \sum_{\delta=1}^{l} \phi \left(P_\delta + \frac{X}{l} - \sum_{i=1}^{l} \frac{P_i}{l} \right) \\ &= \phi \left(\sum_{\delta=1}^{l} P_\delta + \sum_{\delta=1}^{l} \frac{X}{l} + \sum_{\delta=1}^{l} \sum_{i=1}^{l} \frac{P_i}{l} \right) \\ &= \phi \left(\sum_{\delta=1}^{l} P_\delta - \sum_{i=1}^{l} P_i + X \right) = \phi X. \quad (28) \end{aligned}$$

From (27) and (28) it follows that

$$\begin{aligned} \dot{V} \leq &\sum_{i=1}^{l} \rho_i \Big\{ e^T P_i \dot{e} + \dot{e}^T P_i e + e^T \phi X e + e^T N^T \dot{e} + \dot{e}^T N^T e \\ &- e^T (NA_i + A_i^T N^T) e - e^T N B_i u - u^T B_i^T N^T e \\ &+ \dot{e}(O + O^T) \dot{e} - \dot{e}^T O A_i e - e^T A_i^T O^T \dot{e} - \dot{e}^T O B_i u \\ &- u^T B_i^T O^T \dot{e} + u^T K \dot{e} + \dot{e}^T K^T u - u^T K A_i e - e^T A_i^T K^T u \\ &- u(KB_i + B_i^T K^T) u + e^T GI u + u^T I^T G^T e \\ &+ e^T (GIF_i + F_i^T I^T G^T) e + \dot{e}^T \sigma GI u + u^T \sigma I^T G^T \dot{e} \\ &+ \dot{e}^T \sigma GIF_i e + e^T \sigma F_i^T I^T G^T \dot{e} + u^T \mu(I + I^T) u \\ &+ u^T \mu IF_i e + e^T \mu F_i^T I^T u \Big\} \\ = &\sum_{i=1}^{l} \rho_i \begin{bmatrix} e^T & \dot{e}^T & u^T \end{bmatrix} \psi_i \begin{bmatrix} e^T & \dot{e}^T & u^T \end{bmatrix}^T. \quad (29) \end{aligned}$$

Since $\rho_i \geq 0$, (29) is positive definite if $\psi < 0$. Defining $S_i = IF_i$ and substituting the result into ψ_i, the LMI (24) is obtained. The proof is completed. ∎

5. Distributed control

The graph of the multiagent system in question is shown in Fig. 3. Assuming that the lead agent is governed by the control law of (20), the following control laws are proposed for the follower agents:

$$\dot{\varphi}_i(t) = \sum_{j=1}^{N} a_{ij}(\varphi_j(t) - \varphi_i(t))$$
$$+ m_i(\varphi_0(t) - \varphi_i(t)), \qquad (30)$$

$$\dot{v}_i(t) = \sum_{j=1}^{N} a_{ij}(v_j(t) - v_i(t))$$
$$+ m_i(v_0(t) - v_i(t)), \qquad (31)$$

with $i = 1, \ldots, N$ and where the terms a_{ij} are the edge weights of the graph in Fig. 3; m_i's are the fixed gains of the agents that receive information directly from the leader; (φ_i, v_i) belongs to the agent that receives the information and (φ_j, v_j) belongs to the one that sends it; finally, (φ_0, v_0) are the state and input associated with the lead agent. Expanding (30), we get

$$\dot{\varphi}_i(t) = \sum_{j \in N_i} a_{ij}(\varphi_j(t) - \varphi_i(t)) + m_i(\varphi_0(t) - \varphi_i(t))$$

$$= -\varphi_i(t) \sum_{j \in N_i} a_{ij} + \sum_{j \in N_i} a_{ij}\varphi_j(t) + m_i\varphi_0(t)$$

$$- m_i\varphi_i(t)$$

$$= -d_i\varphi_i(t) + \begin{bmatrix} a_{i1} & \ldots & a_{iN} \end{bmatrix} \begin{bmatrix} \varphi_1(t) \\ \vdots \\ \varphi_N(t) \end{bmatrix}$$

$$+ \begin{bmatrix} m_1 & \ldots & m_N \end{bmatrix} \begin{bmatrix} \varphi_0(t) \\ \vdots \\ \varphi_0(t) \end{bmatrix}$$

$$- \begin{bmatrix} m_1 & \ldots & m_N \end{bmatrix} \begin{bmatrix} \varphi_1(t) \\ \vdots \\ \varphi_N(t) \end{bmatrix}, \qquad (32)$$

where d_i is the number of edges that reach agent i. Thus, with the diagonal matrix of the graph D, the global angular velocity dynamics can be obtained:

$$\dot{\varphi}(t) = -D\varphi(t) + W\Phi(t) + M\Phi_0(t) - M\Phi(t)$$
$$= -(D - W)\Phi(t) + M\Phi_0(t) - M\Phi(t)$$
$$= -L\Phi(t) + M\Phi_0(t) - M\Phi(t) \qquad (33)$$
$$= -(L + M)\Phi(t) + M\Phi_0(t),$$

where the leader's state is

$$\Phi_0(t) = \begin{bmatrix} \varphi_0(t) & \ldots & \varphi_0(t) \end{bmatrix}^T,$$

with appropriate dimensions, and

$$\Phi(t) = \begin{bmatrix} \varphi_1(t) & \ldots & \varphi_N(t) \end{bmatrix}^T \in \mathbb{R}^N.$$

Similarly, for the input $v_i(t)$ in (31) with

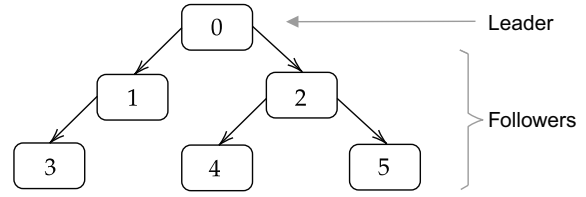$$\Upsilon_0(t) = \begin{bmatrix} v_0(t) & \ldots & v_0(t) \end{bmatrix}^T$$

Fig. 4. Graph of the multiagent system for the numerical example.

as the leader's input and

$$\Upsilon(t) = \begin{bmatrix} v_1(t) & \ldots & v_N(t) \end{bmatrix}^T \in \mathbb{R}^N$$

as the global vector of the input, the global linear velocity dynamics can be obtained:

$$\dot{v}(t) = -(L + M)\Upsilon(t) + M\Upsilon_0(t). \qquad (34)$$

Combining (33) and (34), the general control law applied to the follower agents is obtained:

$$\begin{bmatrix} \dot{\varphi}(t) \\ \dot{v}(t) \end{bmatrix} = -(I_n \otimes (L + M)) \begin{bmatrix} \Phi(t) \\ \Upsilon(t) \end{bmatrix}$$
$$+ (I_n \otimes M) \begin{bmatrix} \Phi_0(t) \\ \Upsilon_0(t) \end{bmatrix},$$

where I_n is the identity matrix of dimension $n = 2$, L and M are the matrices associated with the graph, and the symbol $\otimes$ corresponds to the Kronecker product.

6. Results

A numerical example is considered to demonstrate the effectiveness of the proposed methodology. First, the convex controller performance is evaluated on an individual agent who will be the MAS leader. Second, the distributed controller is implemented on five differential robots to follow the leading agent, constituting the leader–follower formation as shown Fig. 4. Similar robots are considered to have a homogeneous MAS.

6.1. Numerical example for the convex control of the leader.
This example demonstrates the control designed for the leading agent represented in the graph with the subscript 0. The objective is to track the desired trajectory represented by a circle of four meters in diameter. The convex model is obtained by evaluating the varying matrices of (18) on the intervals $\zeta_1 \in [-\pi, \pi]$ rad/s, $\zeta_2 \in [0, 0.2]$ m/s, $\zeta_3 \in [-4, 4]$ m, $\zeta_4 \in [-6.5, 4]$ m and $\zeta_5 \in [0.1, 1]$ rad, which relies on 32 local models. Local matrices are not displayed here, but can be obtained by substituting the scheduling parameters ζ on A_i, B_i. These intervals were selected by considering the physical constraints on the robot's
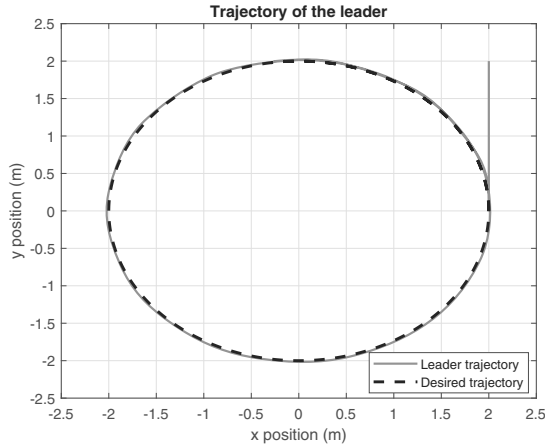
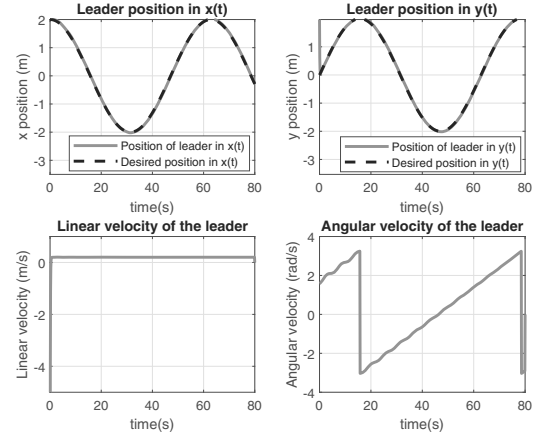Fig. 5. Trajectory made by the leader.

Fig. 6. Position and velocities for the leader.

angular and linear displacements and velocities. After evaluating the controllability of (18), the gain matrices of the control law in (20) are computed by solving the LMIs of Theorem 1 using the SeDuMi solver (Sturm, 1999) and the YALMIP Toolbox (Lofberg, 2004). The following values of μ, ϕ, and σ were considered for the LMI:

$$G = \begin{bmatrix} -700 & 0 \\ 0 & -600 \\ 0 & 0 \end{bmatrix},$$

$$\mu = 10^2, \quad \phi = 10^{-3}, \quad \sigma = 10.$$

The resulting gain matrices are displayed in Appendix. Initial conditions for the position $(x(t), y(t))$ and the orientation $\varphi(t)$ of the robot are $(x(0), y(0), \varphi(0)) = (2, 2, \pi/2)$ for the simulation. The result is shown in Fig. 5. The desired trajectory is depicted with a dashed line, while the path followed by the robot is represented with a solid line. As evident from the results, the agent precisely follows the desired trajectory, achieving a low root-mean-square error (RMS) of just 0.0145 m for the x-axis position and 0.0261 m for the y-axis position. The results demonstrate the effectiveness of the convex controller, which is crucial because the leader describes the desired performance of the followers. Figure 6 shows the time evolution of the vehicle's x and y positions during the validation for the same trajectory. It also offers valuable insights into the essential control inputs. This visualization demonstrates how each axis is effectively stabilized in accordance with the desired reference.

6.2. Distributed control protocol for consensus.
This simulation illustrates the leader–follower performance of the MAS in Fig. 4. The objective is for the leader to perform the desired trajectory, and the five follower agents must follow the leader without knowing

the trajectory. The initial conditions for the followers are $(x_1(0), y_1(0), \varphi_1(0)) = (4, 0, \pi/2)$ for Agent 1; $(x_2(0), y_2(0), \varphi_2(0)) = (0, 0, \pi/2)$ for Agent 2; $(x_3(0), y_3(0), \varphi_3(0)) = (5, -1, \pi/2)$ for Agent 3; $(x_4(0), y_4(0), \varphi_4(0)) = (2, -2, \pi/2)$ for Agent 4; and $(x_5(0), y_5(0), \varphi_5(0)) = (-2, -2, \pi/2)$ for Agent 5. The matrices associated with the graph in Fig. 4 are

$$W = \begin{bmatrix} 0 & 0 & 0 & 0 & 0 \\ 0 & 0 & 0 & 0 & 0 \\ 1 & 0 & 0 & 0 & 0 \\ 0 & 1 & 0 & 0 & 0 \\ 0 & 1 & 0 & 0 & 0 \end{bmatrix},$$

$$D = \begin{bmatrix} 0 & 0 & 0 & 0 & 0 \\ 0 & 0 & 0 & 0 & 0 \\ 0 & 0 & 1 & 0 & 0 \\ 0 & 0 & 0 & 1 & 0 \\ 0 & 0 & 0 & 0 & 1 \end{bmatrix},$$

$$L = \begin{bmatrix} 0 & 0 & 0 & 0 & 0 \\ 0 & 0 & 0 & 0 & 0 \\ -1 & 0 & 1 & 0 & 0 \\ 0 & -1 & 0 & 1 & 0 \\ 0 & -1 & 0 & 0 & 1 \end{bmatrix},$$

$$M = \begin{bmatrix} m_1 & 0 & 0 & 0 & 0 \\ 0 & m_2 & 0 & 0 & 0 \\ 0 & 0 & m_3 & 0 & 0 \\ 0 & 0 & 0 & m_4 & 0 \\ 0 & 0 & 0 & 0 & m_5 \end{bmatrix}$$

$$= \begin{bmatrix} 1 & 0 & 0 & 0 & 0 \\ 0 & 1 & 0 & 0 & 0 \\ 0 & 0 & 0 & 0 & 0 \\ 0 & 0 & 0 & 0 & 0 \\ 0 & 0 & 0 & 0 & 0 \end{bmatrix}.$$

The results are shown in Fig. 7. Every mobile robot faithfully replicates the leader's trajectory and maintains the formation, showcasing the efficiency of the proposed
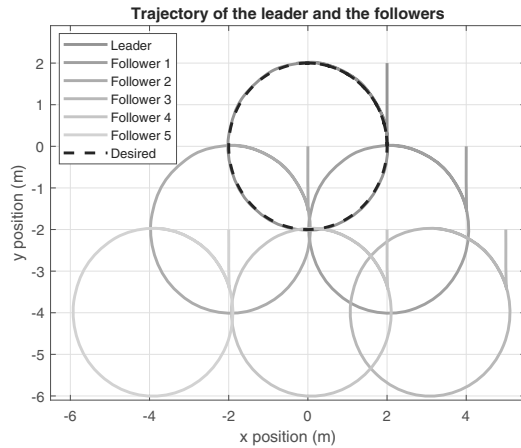
Fig. 7. Trajectories made by the leader and followers.

Fig. 8. Consensus of all robots.

approach. It should be emphasized that only the leading agent possesses the knowledge of the trajectory, whereas the subsequent agents rely exclusively on information exchanged with their neighboring agents. In this case, Agents 1 and 2 receive the velocity data from the leader, Agents 3 and 4 receive information from Agent 1, and Agent 5 from Agent 2. The virtual simulation can be consulted at `https://youtu.be/V1l_6Qv7rKQ`. As can be observed, all robots maintain the desired formation and orientation. Figure 8 provides a visualization of the consensus achieved regarding each robot's linear velocity and orientation. Notably, the linear velocities of all the robots converge to the same value and remain stable throughout the simulation. A minor steady-state error in orientation is observed primarily because the leader adheres to a circular reference, causing continuous changes in the orientation values.

It is important to note that this research deals with the challenging problem of achieving convex control for nonholonomic systems by considering a realistic nonlinear kinematic model, unlike most existing works that rely on linear models or simplified numerical examples. This issue is of primary importance because the nonholonomic nature poses some controllability problems from the theoretic point of view, which are solved by splitting the controllable and the uncontrollable parts. Nevertheless, it is essential to acknowledge the limitations of our method. For instance, robustness to measurement noise and external disturbances remains an area of concern, potentially diminishing its practical applicability. This is a critical point for improvement, and future work will address this challenge, enhancing our approach's overall efficacy and utility. Also, there is an implicit assumption that agent communication is ideal, i.e., no delays, data loss, etc. are considered. In such cases, additional strategies not covered in this work are required.
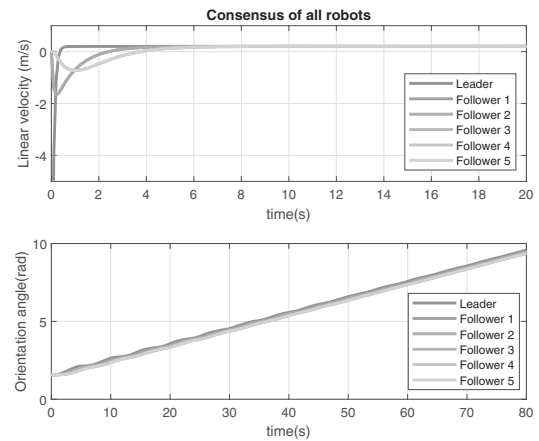
7. Conclusions

In this work, a convex control scheme for the leading differential robot of a multiagent system of five mobile follower robots using non-quadratic Lyapunov functions was designed for the follower robots, and distributed control protocols are used for the leader–follower consensus. These algorithms manage to control the states of the agents in the formation and follow predefined trajectories (in this case, a circle with a diameter of four meters). The controller gain matrices guarantee the asymptotic convergence of the following error. However, the results also revealed crucial areas for further development and enhancement; to practically implement the consensuses protocol, it is essential to consider robustness against sensor noise, external disturbances, and uncertainties that arise from real-world robots and obstacle avoidance capabilities. Future work will incorporate H_∞ performance criteria and trajectory planning (Liu *et al.*, 2022) to reach these goals.

Acknowledgment

References

Abdulwahhab, O.W. and Abbas, N.H. (2018). Design and stability analysis of a fractional order state feedback controller for trajectory tracking of a differential drive robot, *International Journal of Control, Automation and Systems* **16**(6): 2790–2800.

Ahmed, I., Rehan, M., Iqbal, N. and Ahn, C.K. (2023). A novel event-triggered consensus approach for generic linear multi-agents under heterogeneous sector-restricted input nonlinearities, *IEEE Transactions on Network Science and Engineering* **10**(3): 1648–1658.

Ahsan Razaq, M., Rehan, M., Tahir, F. and Chadli, M. (2020). H_∞ leader-based consensus of non-linear multi-agents over switching graphs and disturbances using multiple Lyapunov functions, *IET Control Theory & Applications* **14**(20): 3395–3405.

Ai, X. and Wang, L. (2021). Distributed fixed-time event-triggered consensus of linear multi-agent systems with input delay, *International Journal of Robust and Nonlinear Control* **31**(7): 2526–2545.

Amirkhani, A. and Barshooi, A.H. (2022). Consensus in multi-agent systems: A review, *Artificial Intelligence Review* **55**(5): 3897–3935.

Attallah, A. and Werner, H. (2020). Information flow in formation control for nonholonomic agents modeled as LPV systems, *2020 European Control Conference (ECC), St. Petersurg, Russia*, pp. 459–464.

Bernal, M., Estrada, V. and Márquez, R. (2019). *Diseno e implementación de sistemas de control basados en estructuras convexas y desigualdades matriciales lineales*, Pearson, Mexico City.

Blažič, S. and Bernal, M. (2011). Trajectory tracking for nonholonomic mobile robots based on extended models, *IFAC Proceedings Volumes* **44**(1): 5938–5943.

Corke, P. (2017). *Robotics, Vision and Control: Fundamental Algorithms in MATLAB®*, 2nd Edn, Springer, Cham.

Dian, S., Han, J., Guo, R., Li, S., Zhao, T., Hu, Y. and Wu, Q. (2019). Double closed-loop general type-2 fuzzy sliding model control for trajectory tracking of wheeled mobile robots, *International Journal of Fuzzy Systems* **21**(7): 2032–2042.

Gong, S., Zheng, M., Hu, J. and Zhang, A. (2023). Event-triggered cooperative control for high-order nonlinear multi-agent systems with finite-time consensus, *International Journal of Applied Mathematics and Computer Science* **33**(3): 439–448, DOI: 10.34768/amcs-2023-0032.

González-Sierra, J., Aranda-Bricaire, E., Rodríguez-Cortés, H. and Santiaguillo-Salinas, J. (2021). Formation tracking for a group of differential-drive mobile robots using an attitude observer, *International Journal of Control* **94**(1): 89–102.

Lendek, Z., Guerra, T.M., Babuska, R. and De Schutter, B. (2011). *Stability analysis and Nonlinear Observer Design Using Takagi–Sugeno Fuzzy Models*, Springer, Berlin.

Lewis, F.L., Zhang, H., Hengster-Movric, K. and Das, A. (2013). *Cooperative Control of Multi-Agent Systems: Optimal and Adaptive Design Approaches*, Springer, London.

Liu, G., Wu, S., Zhu, L., Wang, J. and Lv, Q. (2022). Fast and smooth trajectory planning for a class of linear systems based on parameter and constraint reduction, *International Journal of Applied Mathematics and Computer Science* **32**(1): 11–21, DOI: 10.34768/amcs-2022-0002.

Liu, Y., Li, T., Shan, Q., Yu, R., Wu, Y. and Chen, C.P. (2020). Online optimal consensus control of unknown linear multi-agent systems via time-based adaptive dynamic programming, *Neurocomputing* **404**(1): 137–144.

Lofberg, J. (2004). YALMIP: A toolbox for modeling and optimization in Matlab, *IEEE International Conference on Robotics and Automation, Taipei, Taiwan*, pp. 284–289.

Manoharan, S.H. and Chiu, W.-Y. (2019). Consensus based formation control of automated guided vehicles using dynamic destination approach, *58th Annual Conference of the Society of Instrument and Control Engineers of Japan (SICE), Hiroshima, Japan*, pp. 902–907.

Miao, Z., Liu, Y.-H., Wang, Y., Yi, G. and Fierro, R. (2018). Distributed estimation and control for leader-following formations of nonholonomic mobile robots, *IEEE Transactions on Automation Science and Engineering* **15**(4): 1946–1954.

Moradi, M., Safarinejadian, B. and Shafiei, M. (2022). H_∞ smooth switching distributed consensus controller for uncertain time-delay switched LPV multi-agent systems, *Transactions of the Institute of Measurement and Control* **44**(12): 2454–2471.

Moreno-Valenzuela, J., Montoya-Villegas, L.G., Pérez-Alcocer, R. and Rascón, R. (2022). Saturated proportional-integral-type control of UWMRS with experimental evaluations, *International Journal of Control, Automation and Systems* **20**(1): 184–197.

Nuno, E., Loria, A., Hernández, T., Maghenem, M. and Panteley, E. (2020). Distributed consensus-formation of force-controlled nonholonomic robots with time-varying delays, *Automatica* **120**(1): 109114.

Ollervides-Vazquez, E.J., Rojo-Rodriguez, E.G., Garcia-Salazar, O., Amezquita-Brooks, L., Castillo, P. and Santibañez, V. (2020). A sectorial fuzzy consensus algorithm for the formation flight of multiple quadrotor unmanned aerial vehicles, *International Journal of Micro Air Vehicles* **12**: 1–24.

Razaq, M.A., Rehan, M., Hussain, M., Ahmed, S. and Hong, K. (2023). Observer-based leader-following consensus of one-sided Lipschitz multi-agent systems over input saturation and directed graphs, *Asian Journal of Control* **25**(5): 4096–4112.

Rehan, M., Ahn, C.K. and Chadli, M. (2019). Consensus of one-sided Lipschitz multi-agents under input saturation, *IEEE Transactions on Circuits and Systems II: Express Briefs* **67**(4): 745–749.

Saadabadi, H. and Werner, H. (2021). Event-triggered ℓ_2 optimal formation control for agents modeled as LPV systems, *IEEE Conference on Decision and Control (CDC), Austin, USA*, pp. 1256–1262.

Sturm, J.F. (1999). Using SeDuMi 1.02, A Matlab toolbox for optimization over symmetric cones, *Optimization Methods and Software* **11**(1–4): 625–653.

Subiantoro, A., Hadi, M.S.A. and Muis, A. (2020). Distributed linear parameter varying model predictive controller with event-triggered mechanism for nonholonomic mobile

robot, *International Conference on Advances in the Emerging Computing Technologies (AECT), Al Madinah Al Munawwarah, Saudi Arabia*, pp. 1–6.

Vafamand, N. and Shasadeghi, M. (2017). More relaxed non-quadratic stabilization conditions using TS open loop system and control law properties, *Asian Journal of Control* **19**(2): 467–481.

Wu, X., Wang, S. and Xing, M. (2018). Observer-based leader-following formation control for multi-robot with obstacle avoidance, *IEEE Access* **7**(1): 14791–14798.

Yao, P., Wei, Y. and Zhao, Z. (2022). Null-space-based modulated reference trajectory generator for multi-robots formation in obstacle environment, *ISA Transactions* **123**(1): 168–178.

Zakwan, M. and Ahmed, S. (2019). Distributed output feedback control of decomposable LPV systems with delay: Application to multi-agent nonholonomic systems, *European Control Conference (ECC), Naples, Italy*, pp. 2899–2903.

Zhang, J., Zhang, H., Sun, S. and Gao, Z. (2021). Leader–follower consensus control for linear multi-agent systems by fully distributed edge-event-triggered adaptive strategies, *Information Sciences* **555**(1): 314–338.

Zhang, S., Zhang, T., Guo, H. and Zhang, F. (2022). General attitude cooperative control of satellite formation by set stabilization, *Acta Astronautica* **191**(1): 125–133.

Zhu, F. and Tan, C. (2023). Consensus control of linear parameter-varying multi-agent systems with unknown inputs, *Sensors* **23**(11): 5125.

Francisco-Ronay López-Estrada holds a PhD degree from the University of Lorraine, France. Since 2008, he has been with Tecnológico Nacional de México, IT Tuxtla Gutiérrez. He is the author of over 70 papers. His research interests focus on fault diagnosis and fault-tolerant control based on convex LPV and Takagi–Sugeno models. He is a member of the editorial boards of *Mathematical and Computational Applications* and the *International Journal of Applied Mathematics and Computer Science*.

Helen Darias received her MSc degree in mechatronics from Tecnológico Nacional de México, IT Tuxtla Gutiérrez, in 2022. Her research interests are in multiagent systems, LPV systems, and robotic systems.

Vicenç Puig holds a PhD in automatic control, vision, and robotics from Universitat Politécnica de Catalunya · Barcelona Tech (UPC). He is a full professor at the Automatic Control Department of UPC and a researcher at the Institute of Robotics and Industrial Informatics, CSIC–UPC. He is the director of the Automatic Control Department and the head of the Research Group on Advanced Control Systems at UPC. He has made important scientific contributions in the areas of fault diagnosis and fault-tolerant control, using interval and linear-parameter-varying models exploiting set-based approaches.

Guillermo Valencia-Palomo holds a PhD degree from the University of Sheffield, UK. Since 2010, he has been with Tecnológico Nacional de México, IT Hermosillo. He is an author of over 70 papers. His research interests include LPV systems, fault diagnosis, and fault-tolerant control. He is an associate editor of *IEEE Access*, the *International Journal of Aerospace Engineering*, *IEEE Latin America Transactions*, and a member of the editorial board of *Mathematical and Computational Applications*.

Joaquín Domínguez-Zenteno received his PhD degree from TENAM University, Mexico, in 2022. Since 2006, he has been with Tecnológico Nacional de México, IT Tuxtla Gutierrez. His research interests are in multiagent systems, mobile robotics, automatic control, and mechatronic systems.

María-Eusebia Guerrero-Sánchez holds a PhD degree from the National Center for Research and Technological Development in Mexico. She has held post-doctoral positions at the French-Mexican Laboratory on Computer Science and Control UMI–LAFMIA at CINVESTAV, Mexico. She is now with Tecnológico Nacional de México, IT Hermosillo. Her research interests are focused on multiagent systems, passivity-based control, nonlinear control, and UAVs.

Appendix

Gain matrices

Gain matrices K_1 to K_{32} obtained for the example:

$$\begin{bmatrix} -6.950 & 0.190 & 0.0008 \\ -0.020 & -6.238 & -0.0015 \end{bmatrix}, \begin{bmatrix} -6.951 & 0.190 & 0.0007 \\ -0.020 & -6.237 & -0.0015 \end{bmatrix},$$

$$\begin{bmatrix} -6.950 & 0.187 & 0.0007 \\ -0.018 & -5.855 & 0.0010 \end{bmatrix}, \begin{bmatrix} -6.950 & 0.187 & 0.0007 \\ -0.018 & -5.855 & 0.0009 \end{bmatrix},$$

$$
\begin{bmatrix} -6.952 & -0.146 & -0.0011 \\ -0.019 & -6.237 & -0.0014 \end{bmatrix},
\begin{bmatrix} -6.952 & -0.146 & -0.0011 \\ -0.019 & -6.237 & -0.0014 \end{bmatrix},
$$

$$
\begin{bmatrix} -6.952 & -0.144 & -0.0013 \\ -0.018 & -5.855 & 0.0008 \end{bmatrix},
\begin{bmatrix} -6.952 & -0.144 & -0.0013 \\ -0.018 & -5.855 & 0.0008 \end{bmatrix},
$$

$$
\begin{bmatrix} -6.950 & 0.190 & 0.0008 \\ -0.020 & -6.238 & -0.0027 \end{bmatrix},
\begin{bmatrix} -6.951 & 0.190 & 0.0007 \\ -0.020 & -6.237 & -0.0027 \end{bmatrix},
$$

$$
\begin{bmatrix} -6.950 & 0.187 & 0.0008 \\ -0.018 & -5.855 & -0.0002 \end{bmatrix},
\begin{bmatrix} -6.950 & 0.187 & 0.0007 \\ -0.018 & -5.855 & -0.0003 \end{bmatrix},
$$

$$
\begin{bmatrix} -6.952 & -0.146 & -0.0011 \\ -0.019 & -6.237 & -0.0026 \end{bmatrix},
\begin{bmatrix} -6.952 & -0.146 & -0.0011 \\ -0.019 & -6.237 & -0.0026 \end{bmatrix},
$$

$$
\begin{bmatrix} -6.952 & -0.144 & -0.0013 \\ -0.018 & -5.855 & -0.0004 \end{bmatrix},
\begin{bmatrix} -6.952 & -0.144 & -0.0013 \\ -0.018 & -5.855 & -0.0004 \end{bmatrix},
$$

$$
\begin{bmatrix} -6.951 & 0.146 & 0.0008 \\ 0.018 & -6.238 & -0.0015 \end{bmatrix},
\begin{bmatrix} -6.951 & 0.146 & 0.0007 \\ 0.018 & -6.237 & -0.0015 \end{bmatrix},
$$

$$
\begin{bmatrix} -6.951 & 0.144 & 0.0008 \\ 0.019 & -5.855 & 0.0009 \end{bmatrix},
\begin{bmatrix} -6.951 & 0.144 & 0.0008 \\ 0.019 & -5.855 & 0.0008 \end{bmatrix},
$$

$$
\begin{bmatrix} -6.952 & -0.190 & -0.0012 \\ 0.018 & -6.237 & -0.0014 \end{bmatrix},
\begin{bmatrix} -6.952 & -0.190 & -0.0011 \\ 0.018 & -6.237 & -0.0014 \end{bmatrix},
$$

$$
\begin{bmatrix} -6.952 & -0.188 & -0.0013 \\ 0.019 & -5.855 & 0.0008 \end{bmatrix},
\begin{bmatrix} -6.952 & -0.188 & -0.0013 \\ 0.019 & -5.855 & 0.0007 \end{bmatrix},
$$

$$
\begin{bmatrix} -6.951 & 0.146 & 0.0008 \\ 0.018 & -6.238 & -0.0027 \end{bmatrix},
\begin{bmatrix} -6.951 & 0.146 & 0.0007 \\ 0.018 & -6.237 & -0.0027 \end{bmatrix},
$$

$$
\begin{bmatrix} -6.951 & 0.144 & 0.0008 \\ 0.019 & -5.855 & -0.0003 \end{bmatrix},
\begin{bmatrix} -6.951 & 0.144 & 0.0008 \\ 0.019 & -5.855 & -0.0004 \end{bmatrix},
$$

$$
\begin{bmatrix} -6.952 & -0.189 & -0.0012 \\ 0.018 & -6.237 & -0.0026 \end{bmatrix},
\begin{bmatrix} -6.952 & -0.190 & -0.0011 \\ 0.018 & -6.237 & -0.0026 \end{bmatrix},
$$

$$
\begin{bmatrix} -6.952 & -0.188 & -0.0013 \\ 0.019 & -5.855 & -0.0004 \end{bmatrix},
\begin{bmatrix} -6.952 & -0.188 & -0.0013 \\ 0.019 & -5.855 & -0.0005 \end{bmatrix}.
$$